

Sand wavelets in laminar open-channel flows

“Ondelettes de sable” dans des écoulements laminaires à ciel ouvert

STEPHEN E. COLEMAN, *Senior Lecturer, Department of Civil and Resource Engineering, The University of Auckland, Private Bag 92019, Auckland, New Zealand. Email: s.coleman@auckland.ac.nz*

BURKHARD ELING, *Cand. Ing. Oec., Technical University of Braunschweig, Braunschweig, Germany*

ABSTRACT

The results of experimental investigations indicate that sand wavelets can be generated from plane-bed conditions in open-channel laminar flow, the lengths, shapes and patterns of generation for these wavelets being consistent with observations for alluvial flows. Wavelets are of a preferred wavelength which is relatively insensitive to the characteristics of the applied flow and primarily a function of the size of the sediment, these wavelengths λ for alluvial and laminar open-channel flows over beds of quartz and lightweight sediments of size $d = 0.2$ mm to $d = 1.6$ mm being simply described by $\lambda = 175d^{0.75}$, where λ and d are expressed in millimetres. The laminar-flow sand-wavelet data present significant implications to contemporary understanding of bed-form mechanics, with both ripples and dunes being postulated to subsequently develop from these wavelets for alluvial flows. The data also raise significant questions as to whether the generation of ripples and dunes in alluvial flows can be attributed to an organised structure of turbulence within the flow.

RÉSUMÉ

Les résultats des études expérimentales montrent que des "ondélettes de sable" peuvent apparaître, en partant des conditions initiales du fond plat, dans des écoulements laminaires à ciel ouvert. Les longueurs, les formes et la disposition générale des ondélettes sont consistantes avec les observations des écoulements alluviaux. Les ondélettes sont caractérisées par une longueur d'onde préférentielle relativement indépendante des conditions de l'écoulement et dépendante surtout des dimensions des sédiments. Pour les écoulements alluviaux et laminaires à ciel ouvert sur des lits composés de quartz et des sédiments légers de diamètres entre $d = 0,2$ mm et $d = 1,6$ mm cette longueur d'onde peut être définie comme $\lambda = 175d^{0.75}$, où λ et d sont exprimés en millimètres. Les données concernant les ondélettes de sable dans l'écoulement laminaire sont importantes pour la compréhension de la mécanique des formes de lits alluvionnaires. En effet, on postule actuellement que les formes de lit alluviaux telles que les rides, ainsi que les dunes se développent postérieurement et à partir des ondélettes de sable. Les données soulèvent aussi des questions importantes au sujet de la génération des rides et des dunes dans des écoulements alluviaux, à savoir, dans quelle mesure cette génération peut être due aux structures organisées de la turbulence à l'intérieur de l'écoulement.

Introduction

Coleman and Melville (1996) define the waves first generated on a plane bed for a subcritical alluvial flow as wavelets, bed forms (dunes or ripples) subsequently developing from these wavelets (Figure 1).

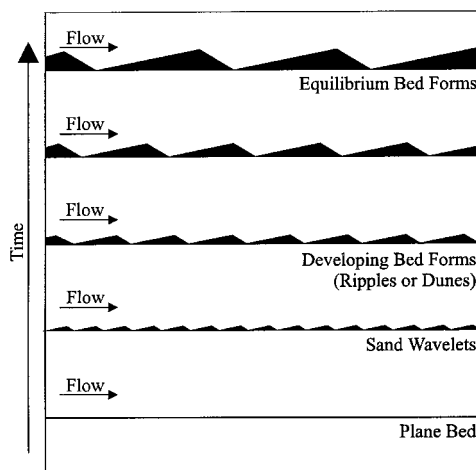


Fig. 1. Schematic of sand-wave development from plane-bed conditions.

Yalin (1992) ascribes the formation of alluvial dunes and bars to bursting processes associated with the turbulent nature of the flow. Raudkivi and Witte (1990) contend that since no ripples

are formed in laminar flow, then initiation of these bed forms must also be a function of turbulence, Raudkivi (1997) further proposing that the initiation of ripples can probably be ascribed to turbulent bursting processes that exhibit certain orders. In contrast, Yalin (1992) concludes that ripples are due to the viscous structures at the bed, defining ripples as the bed forms 'imprinted' by the viscous flow structures (undulations) at the bed of a nevertheless turbulent flow. The view that ripples and dunes can form only in turbulent flow is attributed by Yalin (1972) primarily to the experimental work of Tison (1949), who carried out a series of experiments to determine whether ripple-marks can be generated in uniform laminar flow. Yalin comments, however, that the experiments of Tison (1949) cannot be regarded as exhaustive, and that while dunes can only form in turbulent flow, it is conceivable that ripples could possibly form in laminar flow.

The Tison (1949) experiments utilised a 0.1 m wide tilting flume, with flow depths of 0.02 m to 0.1 m, flow surface velocities of 0.005 m/s to 1 m/s, fluid kinematic viscosities $\nu = 26 \times 10^{-6}$ m²/s to 61×10^{-6} m²/s, and a channel bed of a 'well-calibrated' sand, the grains having dimensions varying from one test to another between 0.06 mm and 5 mm. All flows were of channel Reynolds number $Re = 4U_{ave}r/\nu$ less than 2000, where U_{ave} is average velocity, r is channel hydraulic radius, and $Re < 2000$ indicates laminar flow for which fluid viscosity effects dominate flow inertia effects. A sand fillet of about

Revision received July, 1999. Open for discussion till April 30, 2001.

0.01 m height placed perpendicular to the flow across the channel width generated a flattened undulation downstream of the fillet, but no other apparent waves were generated. The two undulations flattened with time, never adopting the characteristic ripple-mark shape, and eventually disappeared. In separate experiments, flow around an upright prismatic obstacle placed on the flow centreline generated typical erosion around the obstacle, but did not result in a series of waves being generated downstream of the obstacle. Based on these experiments, the author concludes that ripple-marks cannot be generated in laminar flow.

Acknowledging the plethora of examples of waves forming at the interface between two deformable bodies, finding no evidence in the literature of stable sand waves being generated in laminar open-channel flow, recognising a commonly held belief that the generation of ripples and dunes is attributable to turbulence phenomena, and desiring to address the conjecture of Yalin that ripples could possibly form in laminar flow, initial investigations were undertaken at The University of Auckland, New Zealand, to determine if any waves could be generated for laminar open-channel flow over a sand bed (Twose, 1996). Seven experiments were carried out for which the bed sediment was in motion and the flow was laminar, the channel Reynolds number $Re = 4U_{ave}r/\nu$ being less than a maximum value of 1030 for these experiments, where U_{ave} is depth-averaged centreline velocity.

For five of these seven experiments, antidunes were generated downstream of the fixed-bed-deformable-bed discontinuity occurring at the upstream limit of the sediment bed (Coleman et al., 1998). For one experiment, low-amplitude waves in the sediment bed were measured after a period of about 1 hour for the subcritical flow (Coleman et al., 1998). For the remaining run of median sediment size $d_{50} = 0.95$ mm, no bed forms were observed. This latter result has been attributed to having relied solely on coarse visual observations through the depth of the column of translucent oil to determine the presence of any bed forms; the short (approximately 15-minute) duration of the experiment; the low shear stress ratio for this run ($\theta/\theta_c = 1.17$, where θ is dimensionless shear stress and θ_c is dimensionless critical shear stress); and alluvial flow indications that bed forms are possibly not expected to form for this flow of centreline Froude number $Fr = U_{ave}/(gh)^{0.5} = 0.85$, where g is gravitational acceleration and h is flow depth.

Having determined that sand waves could develop and remain stable for subcritical laminar open-channel flows, experiments were subsequently devised to enable investigation of the generation of sand wavelets (Figure 1) from plane-bed conditions for these flows. In carrying out these experiments, it was intended to determine whether laminar-flow sand wavelets are comparable to those generated for turbulent open-channel flows, and if so, to address the aforementioned conjecture of Yalin (1972) that ripples can form in laminar flow, and also to assess the possible implications to contemporary understandings of the generation of waves in sediment beds.

Sand-wave generation experiments

The present open-channel experiments were carried out in a tilting flume of glass side-walls measuring $0.3 \text{ m} \times 0.1 \text{ m}$ (wide) \times 2.55 m (long) (Figure 2). A recess in the wooden channel base measuring $0.025 \text{ m} \times 0.1 \text{ m}$ (wide) \times 1.3 m (long) was filled with sediment to create an erodible bed section. Sediment was not recirculated. The centrifugal pump circulating the flow was controlled using a variable speed drive, vertical sluice gates installed at the upstream and downstream ends of the channel aiding control of flow within the channel. The fluid used in the experiments was Shell Tellus Grade 32 hydraulic oil. For the temperature range of the present experiments, the fluid density could be taken to be essentially constant at $\rho = 870 \text{ kg/m}^3$. The kinematic viscosity, ν , of the oil was available in chart form as a function of temperature in degrees Celsius T .

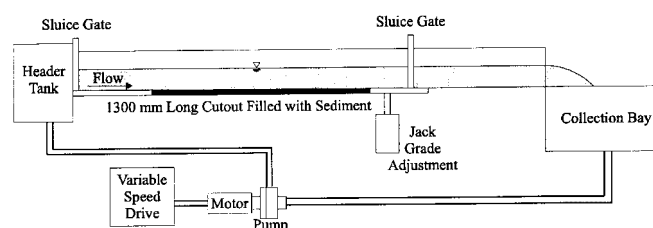


Fig. 2. Schematic of experimental set-up.

A series of six uniform flows was established and measured for a fixed-bed insert in stead of the erodible sediment bed within the recess section of the channel. The centreline velocity profile midway along the test section was measured using a laser Doppler anemometer, the channel slope was determined using a surveying level, flow depth and flow uniformity were measured using a ruler on the channel side-wall, and pump speed and fluid temperature were recorded. Centreline values of average velocity U_{ave} and shear velocity at the bed level u_* were determined from the measured velocity profile. The laminar nature of flow for each run was confirmed by $Re < 2000$ for the run. Recorded measurements enabled a given flow to be reproduced when required.

At the start of a bed development run, the bed was smoothed, the settings for the desired flow were established and then the flow was initiated. At selected stages of bed development, the flow was halted and the bed profile was measured with the channel remaining filled with oil. Bed profiles were typically recorded for the plane bed and then at 10–15 minute intervals for a run. After a bed profile was recorded, the flow was then either resumed in the channel or the bed was flattened with the experiment being started from the beginning and run to a later stage of development. Tests confirmed that the alternative procedures did not significantly influence the experimental results. All centreline bed profiles were measured using a bed profile measurement system (Coleman, 1997), this system being configured to record bed elevation measurements to within ± 0.4 mm every 1.2 mm along the flume.

The characteristics of the 11 experiments carried out are given in Table 1, where $Re_* = d_g u_* / \nu$ is grain Reynolds number, the

geometric mean sediment size $d_g = (d_{84}d_{16})^{0.5}$, the geometric standard deviation of sediment sizes $\sigma_g = (d_{84}/d_{16})^{0.5}$, s is sediment specific gravity, and d_{16} and d_{84} are the sediment sizes for which 16% and 84% respectively by weight of the sediment is finer. The values of critical shear velocity for sediment entrainment u_{*c} for these experiments have been determined based on the extension of Shields diagram provided by the data of White (1970) (Raudkivi, 1990).

Table 1. Experimental parameters.

Sand ¹	Pump Setting	ν (m ² /s)	u_{*c} (m/s)	h (m)	u^* (m/s)	U_{ave} (m/s)	Fr	Re^2	Re^*
1	275	8.50E-05	0.0207	0.048	0.0461	0.2731	0.40	315	0.16
1	300	9.00E-05	0.0219	0.038	0.0438	0.2756	0.45	264	0.15
1	500	8.50E-05	0.0207	0.061	0.0594	0.3715	0.48	480	0.21
1	550	8.50E-05	0.0207	0.067	0.0598	0.5036	0.62	679	0.21
2	300	9.00E-05	0.0234	0.038	0.0438	0.2756	0.45	264	0.19
2	400	9.00E-05	0.0234	0.045	0.0493	0.3419	0.51	360	0.21
2	500	8.50E-05	0.0221	0.061	0.0594	0.3715	0.48	480	0.27
2	600	8.00E-05	0.0208	0.068	0.0616	0.5185	0.63	747	0.30
3	500	8.50E-05	0.0346	0.061	0.0594	0.3715	0.48	480	0.43
3	550	8.50E-05	0.0346	0.067	0.0598	0.5036	0.62	679	0.43
3	600	8.00E-05	0.0325	0.068	0.0616	0.5185	0.63	747	0.47

¹ Sand 1: $d_{50} = 0.29$ mm, $d_g = 0.30$ mm, $\sigma_g = 1.3$, $s = 2.65$.

Sand 2: $d_{50} = 0.44$ mm, $d_g = 0.39$ mm, $\sigma_g = 1.4$, $s = 2.65$.

Sand 3: $d_{50} = 0.64$ mm, $d_g = 0.61$ mm, $\sigma_g = 1.3$, $s = 2.65$.

² For the present channel, $r = (0.1h)/(0.1+2h)$.

As the oil was circulated by the pump, air was increasingly entrained into the flow. Standard tests of the aerated oil and the oil with no entrained air indicated no detectable difference in the oil viscosity. The experimental procedures were designed to allow for that fact that increasing numbers of small bubbles in the fluid would eventually prevent laser measurement of centreline flow velocities or ultrasonic measurement of bed profiles. Owing to entrained air in the fluid and low amplitudes of generated bed forms, for a number of runs, any generated waves could only be detected by eye when the flume was almost drained of oil.

In order to provide a check on the natures of the respective flows, each of the experimentally measured velocity profiles for the six open-channel flows utilised was compared to the predictions of an analytical expression for steady incompressible uniform laminar flow in a rectangular open channel. This expression was derived assuming laminar flow in an open-channel to be equivalent to the flow in the lower half of a closed-rectangular-conduit, Chorlton (1967) providing an analytical expression for the velocity distribution for this latter flow. The measured and theoretical velocity profiles differed significantly only for the largest two pump settings of 550 and 600, the short channel length resulting in these flows not developing fully, the measured velocities then being less than those indicated by the theoretical expression. All flows were nevertheless laminar in

nature, with $Re < 2000$ for each run. All flow parameters were calculated from measured quantities to ensure applicability to the flows being described.

For each experiment, smoothed recorded bed profiles were used to visualise the development of the bed. Autocorrelation analyses of these bed profiles were used to assess the development of the dominant bed wavelength with time for the run. For several runs, the upstream and downstream ends of the bed profile were excluded from the autocorrelation analyses owing to sediment supply conditions making the bed in these regions not representative of the general bed profile. The scour wave that formed at the upstream end of the erodible test section for a number of test runs was in this manner excluded from bed-wave analyses.

Sand waves

For each experiment involving Sand 1, and for 3 of the 4 experiments involving Sand 2, waves were generated and developed over the entire length of the sediment bed (Figures 3 and 4). The free surface of the laminar flow in each case remained essentially planar. The ratio of $u^*/u_{*c} = 1.9$ for Run 2-300, for which waves were not generated within the run duration of two hours, was the lowest for the four runs of Sand 2. No sand waves were also generated for the three runs of Sand 3. The range of u^*/u_{*c} ratios of 1.7 to 1.9 tested for these runs was very limited, however. Consideration of the bed form heights of Figure 3, nominally 1 to 5 mm (measured crest-to-trough) as the waves grow, reveals why such bed forms were often difficult to detect by eye for the present experiments.

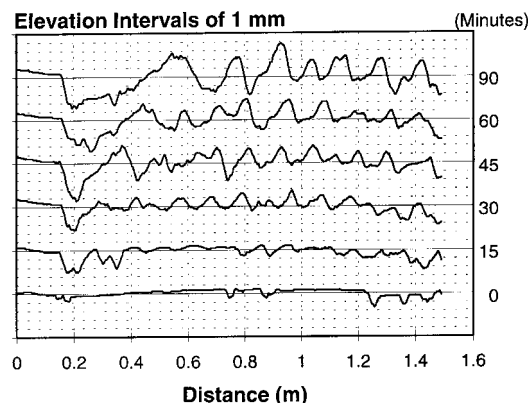


Fig. 3. Sand waves generated for Run 2-500.

The rate of sand-wave generation and development for laminar open-channel flows is markedly slower than that for alluvial flows. This observation is reflected in bed profiles being typically recorded at 10–15 minute intervals for the present experiments of laminar flows (Figure 3). In contrast, for the turbulent open-channel flow experiments of Coleman and Cornelius (1998), bed profiles were typically measured at 15 second intervals in order to record the profiles evidencing the sand wavelets for a run. The relatively slower sand-wave development rates for laminar flows in respect to those for turbulent flows are attributed to the effects of the relative viscosities of these flows.

For both turbulent and laminar flows, however, sand-wave development rate increases with increasing flow strength. Although the three-dimensional shape of the present waves was not a focus of the present investigations, the planform of the present sand waves was observed to resemble a parabola (Figure 4), as would be expected for the laminar nature of the present flows.

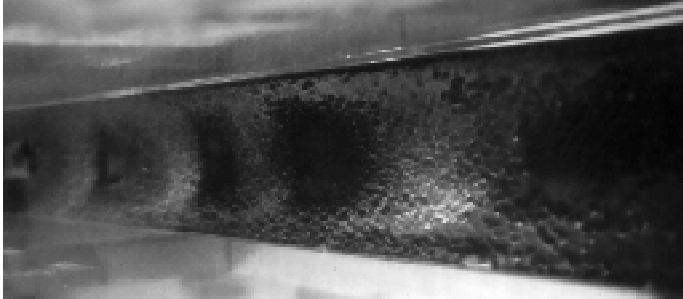


Fig. 4. Sand waves occurring after 90 minutes for Run 2-500, looking down on the channel with flow from left to right.

Sand wavelets

For each of the seven runs for which sand waves developed, the bed profile determined to be that evidencing sand wavelets for the run is shown in Figure 5, sand waves subsequently growing from these wavelets for each run as per the indications of Figure 3. Sand wavelets are defined as the waves first generated on a plane bed, attention not being fixed on a particular time of bed development. The varying times of the bed profiles of Figure 5 then represent when the sand wavelets were first observed from plane bed conditions for the respective runs. Sand wavelets are indicated by the results of Figure 5 to assume (almost instantaneously) a given length, this length subsequently increasing (as per Figure 3) as sand waves evolve from these wavelets. The autocorrelograms corresponding to the bed profiles of Figure 5 are shown as Figure 6. The dominant sand-wavelet lengths λ indicated by the autocorrelograms are summarised in Table 2. Also shown on Figure 5 is a 1.5 m section of the bed profile (after a run duration of 35 seconds) evidencing sand wavelets for Run 3-10 of Coleman and Cornelius (1998). This run, indicated as Run C-3-10-0.58 in Figure 5, involved water flow of $v = 1.17 \times 10^{-6} \text{ m}^2/\text{s}$, $h = 0.19 \text{ m}$, $U_{ave} = 0.613 \text{ m/s}$, $Fr = 0.45$, $Re = 215885$ (for a channel width of 0.45 m), and $u_* = 0.038 \text{ m/s}$ over a sand bed of $d_{50} = 0.43 \text{ mm}$, $d_g = 0.42 \text{ mm}$, $\sigma_g = 1.4$, $u_{*c} = 0.0152 \text{ m/s}$, and $s = 2.63$. The combination of sand and relative shear velocity of $u_* / u_{*c} = 2.5$ for this run is similar to that for Run 2-500 of $u_* / u_{*c} = 2.7$. The dominant sand-wavelet length for the full 3.5 m long bed profile recorded after 35 seconds for Run 3-10 of Coleman and Cornelius (1998) is given in Table 2.

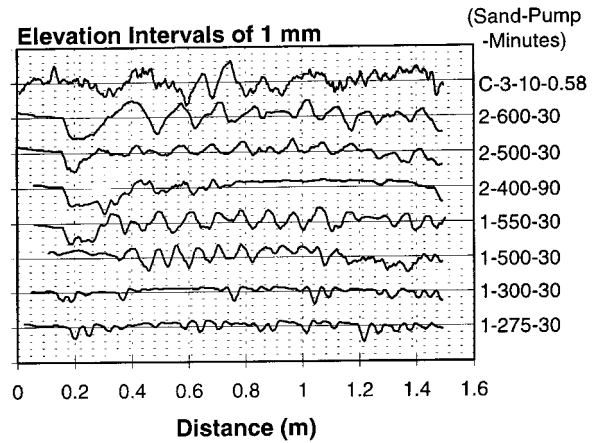


Fig. 5. Bed profiles indicating sand wavelets.

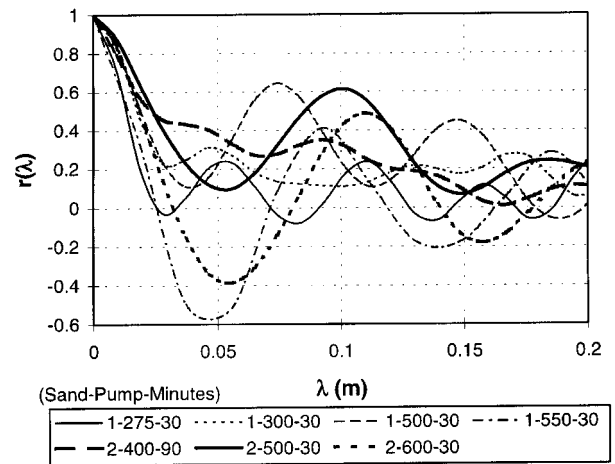


Fig. 6. Autocorrelograms corresponding to the sand-wavelet bed profiles.

Table 2. Sand-wavelet lengths.

Run (Sand-Pump)	Length, λ (m)	Time of Profile (minutes)
1-275	0.052	30
1-300	0.045	30
1-500	0.075	30
1-550	0.093	30
2-300	-	-
2-400	0.092	90
2-500	0.101	30
2-600	0.105	30
3-500	-	-
3-550	-	-
3-600	-	-
C-3-10	0.088	0.58

Owing to a lack of sediment recirculation for the present experiments, a scour hole formed at the upstream end of the erodible test section for a number of runs. This is illustrated by the bed profile at 90 minutes in Figure 3, for which the upstream end of

the erodible bed is located at a distance of approximately 0.16 m. The formation of this scour hole did not adversely influence the generation of sand wavelets for the present runs, with wavelets also being generated either in the absence of or well downstream of this scour hole (Figures 3 and 5). As indicated in Coleman and Melville (1996), sand wavelets in alluvial flows are found to be generated downstream of a discontinuity in the bed, examples of such discontinuities including a fixed-bed-erodible-bed interface or an initial random pile-up of sediment. Sand wavelets in laminar flows are found to be generated in the same fashion (Figures 3 and 5). The general pattern of sand-wave growth and development in laminar flow (once sand wavelets have formed) illustrated in Figure 3 furthermore appears very similar to that apparent for alluvial bed forms, as illustrated in Figure 1 together with the experimental data presented in Figure 4 of Coleman and Melville (1996).

Figure 5 reflects the indication of Table 2 that sand-wavelet lengths are similar across the range of laminar flows tested for a given sediment. These lengths are further similar for both laminar (runs using Sand 2) and turbulent (Run C-3-10) flows over the same sediment.

To further illustrate these findings, the valid alluvial sand-wavelet data summarised by Coleman and Melville (1996) are presented in Figure 7 together with the present sand-wavelet data for laminar flows. For the data of Figure 7, wavelet length normalised by representative sediment size d and critical grain Reynolds number, $Re_{*c} = du_{*c}/\nu$, is plotted as a function of relative shear stress excess, $(\theta - \theta_c)/\theta_c = [(u_*/u_{*c})^2 - 1]$, where dimensionless shear stress $\theta = u_*^2/[(s - 1)gd]$, dimensionless critical shear stress $\theta_c = u_{*c}^2/[(s - 1)gd]$, and the representative sediment size d is equal to d_g , where this is available, or otherwise d_{50} .

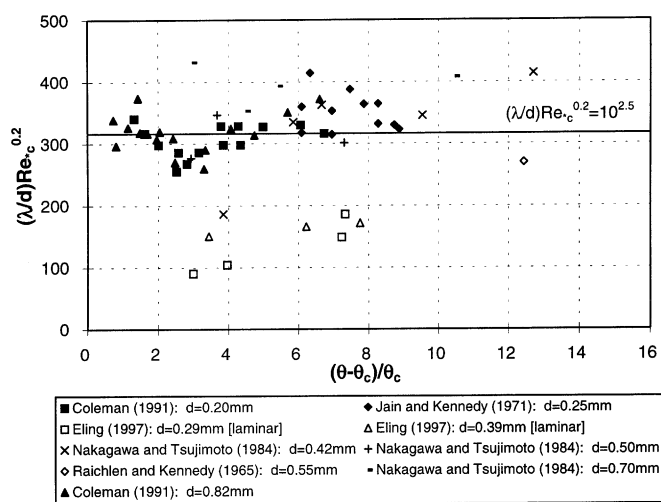


Fig. 7. Variation of normalised sand-wavelet length with relative shear stress excess.

Figure 7 indicates that while the general relation (1) suggested by Coleman and Melville (1996) to describe wavelet lengths is

valid for alluvial sand-wavelet lengths, it is not universally applicable to both laminar and turbulent flows.

$$(\lambda/d)Re_{*c}^{0.2} = 10^{2.5} \quad (1)$$

Based on the indications of Table 2, the data of Figure 7 are presented in Figure 8 with wavelet length normalised solely by representative sediment size d . It can be seen that each series of wavelet data (of sediment of a given size) follows the general trend indicated by the fitted line, both for the alluvial flow data and the laminar flow data. The laminar flow lengths are further the same as those for turbulent flow over the same sediment, as indicated by the respective results of Eling (1997) and Nakagawa and Tsujimoto (1984) for $d \approx 0.4$ mm. The results of Figure 8 confirm for both laminar and turbulent flows the finding of Coleman and Melville (1996) that sand wavelets generated on a sediment bed will be of a preferred wavelength, this length being relatively insensitive to characteristics of the applied flow and primarily a function of the size of the sediment.

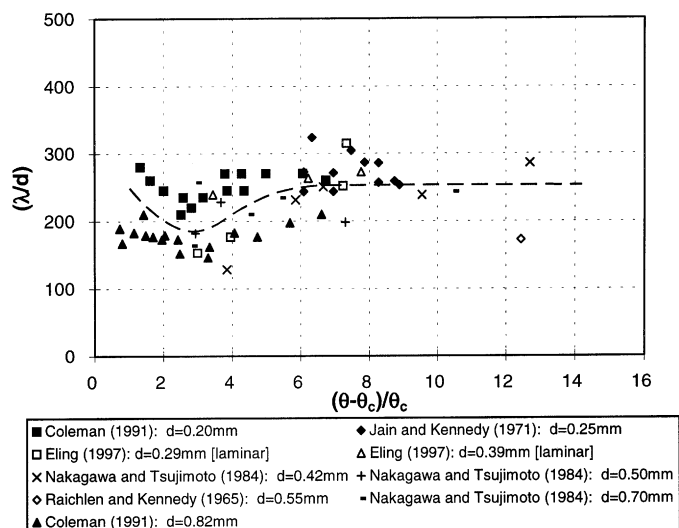


Fig. 8. Variation of sand-wavelet length in terms of sediment size with relative shear stress excess.

Recognising the indications of Figure 8, the relation between wavelet length and sediment size is investigated in Figure 9, for which any dependence of wavelet length on flow characteristics has been ignored. This figure presents the alluvial sand-wavelet data summarised by Coleman and Melville (1996), the present laminar flow sand-wavelet data, and the alluvial sand-wavelet data of Cornelius (1997). These last data, which are presented and discussed further in Coleman and Cornelius (1998), have been included here because they both extend the range of sediment sizes over which alluvial sand wavelets have been measured, and they also provide alluvial sand-wavelet data for a lightweight sediment. The four sediments utilised in the experiments of Cornelius (1997) are of $d_g = 0.42$ mm, 0.85 mm, 0.88 mm and 1.55 mm, $\sigma_g = 1.4, 1.5, 1.2$ and 1.2, and $s = 2.63, 1.85, 2.57$ and 2.61 respectively. The lightweight sediment used was a pumiceous sand.

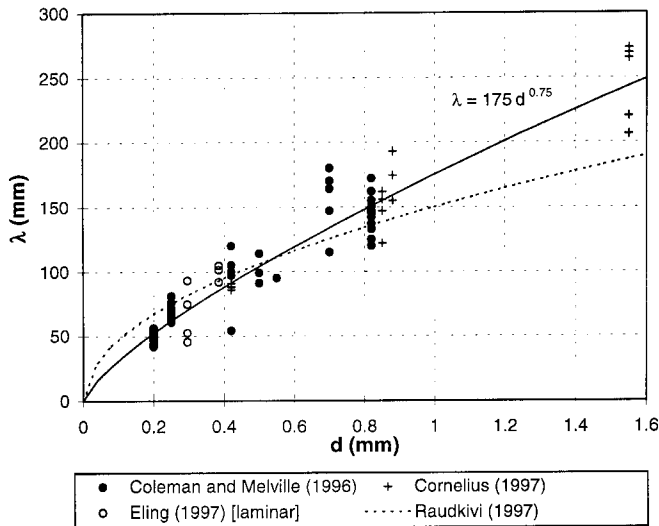


Fig. 9. Sand-wavelet length as a function of sediment size for alluvial and laminar open-channel flows and quartz and lightweight sediments.

The results of Figure 9 indicate that wavelet lengths for both alluvial and laminar open-channel flows and also quartz and lightweight sediments can be reasonably described simply as a function of sediment size. The relation (2) proposed by Raudkivi (1997) for the lengths of initial ripples formed on fine sands is shown on Figure 9, where λ and d are expressed in millimetres. This relation can be seen to approximate the data, although less adequately for smaller and larger sediments. For this relation of (2), λ is indicated to be proportional to $d^{0.5}$, that is, proportional to the fall velocity of the sediment.

$$\lambda \approx 150d^{0.5} \quad (2)$$

Based on regression analyses, an improved simple description of the data of Figure 9 is given by

$$\lambda = 175d^{0.75} \quad (3)$$

A linear relation could also be used to describe variation in wavelet length with sediment size. This relation would be equivalent to (2) and (3), with d raised to the alternative power of unity, although the relation would provide a less adequate fit to the data than (3). Although such a dimensionless relationship describing wavelet length is to be preferred, sand-wavelet data to date clearly conform to a relationship of the form of (3). Future formulation of an appropriate analytical description of the formation of sand wavelets in line with the observed data may help to determine an improved nondimensional expression to describe these data.

The sand-wavelet generation experiments detailed in Coleman and Melville (1996) and Coleman and Cornelius (1998) are of Re_* ranging from 4 to 78. The results of these experiments together with the present results indicate that the same organised wavelets of lengths dependent on the grain size (Figure 9)

form for “rough-boundary” turbulent flows, “hydraulically-smooth” turbulent flows and also laminar flows.

Figure 5 provides a comparison of sand wavelet profiles for laminar flows of $d_g = 0.39$ mm (Sand 2) and a turbulent flow (Run C-3-10) of $d_g = 0.42$ mm. The wavelet profiles for the laminar flows are similar, as would be expected based on the above analyses of wavelet lengths. The wavelet profiles for the turbulent flow are similar to, although perhaps a little steeper than, those for the laminar flows. The increased steepness is accentuated by the ready formation of the separation zone in the bed-form lee for the turbulent flow sand waves, this separation zone and associated region of backflow helping to increase the steepness of the bed-form lee slope.

Implications to the understanding of alluvial bed forms

The diagram of Baas (1993) presented by Raudkivi (1997) for the prediction of the occurrence of various types of alluvial bed forms would predict equilibrium ripple and dune configurations for the alluvial flow experiments of Coleman and Melville (1996) utilising the sediment of $d_g = 0.2$ mm. Equilibrium dune configurations would be predicted for the experiments of Coleman and Melville (1996) utilising the sediment of $d_g = 0.82$ mm. As indicated by the results of Figures 7 to 9, the same sand wavelets formed from plane-bed conditions for the alluvial flow experiments using these two sediments. Based on such observations, Coleman and Melville (1996) contend that both ripples and dunes develop from the same sand wavelets for alluvial flows. Different flow system instability mechanisms, such as the potential flow instability mechanism described by Coleman and Melville (1994) and detailed in Coleman and Fenton (1996), are then postulated to act on these wavelets at subsequent development stages to provide the two separate types of equilibrium bed forms, ripples and dunes, from the same wavelets for these flows.

Sand wavelets are indicated herein to also develop for laminar open-channel flows, the lengths and profiles of these wavelets being directly comparable to those forming for turbulent flows. This result addresses to some extent the conjecture of Yalin (1972) that sand waves in the form of ripples can form in laminar flow. The present measured wavelets are considered herein, however, to provide the seed waves from which both ripples and dunes develop. This is despite sand waves only developing for the present experiments of fine sediments, for which the equilibrium bed forms for alluvial flows are typically ripples. To this end, after run durations of approximately two hours, sand waves had not been generated for the experiments using Sand 3 of $d_g = 0.61$ mm. As indicated earlier, this is postulated to be a result of the limited ranges of flows tested for this sediment. Further tests are required to conclusively determine whether sand wavelets can be generated in laminar flows for coarser sediments, which, based on alluvial flow results, would be expected to form dunes rather than ripples. These experiments should also be run over long durations to effectively assess the possible development of any dune-type bed forms for laminar flows.

With the similarities in the respective sizes, shapes and patterns of generation for sand wavelets in laminar and alluvial flows, a common mechanism appears to be responsible for the generation of both the present laminar sand waves and also alluvial sand waves from plane-bed conditions. The present results, in particular the results of Figures 8 and 9, then raise questions as to whether the initiation of ripples or dunes can be described by theories which predict wavelet lengths to scale with flow characteristics. Common flow instability theories used to describe bed forms need to be reassessed in this regard, as do theories which ascribe sand-wavelet generation to turbulence phenomena, bursting lengths and periods being noted to scale with characteristics of the flow (Raudkivi, 1997). On a more basic level, the noted similarities between the observed laminar and turbulent flow sand wavelets raise principal questions as to whether the generation of sand wavelets in alluvial flows can be attributed to an organised structure of turbulence within the flow. These waves appear more likely to be generated by a form of shear layer instability or an instability of the motion of the granular mass moving over the otherwise plane sediment bed. Further experimental and theoretical investigations are warranted to further assess: the extent to which the present laminar flow sand waves are indeed equivalent to such waves occurring for alluvial flows; and also the implications of the findings of such studies to contemporary understandings of bed-form mechanics.

As indicated earlier, the experiments of Tison (1949), which are similar to those detailed herein, never exhibited any sand waves, introduced bed undulations of 0.01 m height for these experiments not generating a series of undulations downstream but flattening and disappearing with time. It is postulated that the lack of generated sand wavelets for the Tison (1949) runs is due to a limited range of flow conditions being tested for these experiments, as conjectured by Yalin (1972). To this end, the sparse flow details provided by Tison (1949) do not indicate whether the flows tested satisfied the combined criteria necessary for laminar flow sand-wavelet generation of general sediment transport occurring ($\theta/\theta_c > 1$), with $Fr < 1$ and also $Re < 2000$ for the flow (although this last criterion by itself is indicated by the author to hold true for all flows). For each of the present experiments of sand-wavelet generation, these combined criteria are satisfied as required. The degree to which any undulations (of possibly small magnitudes) in bed levels could be detected is also not apparent for the experiments of Tison (1949), the author not specifying any details of the means used to detect and measure variations in bed levels.

Confidence in the present indications that sand waves can be generated and can develop for open-channel laminar flows is provided by the results of Kuru et al. (1995). These authors similarly found that for closed-conduit flows, erodible-bed waves grow from an initially flat surface under laminar flow conditions, turbulence in the carrier fluid not being necessary for the formation of these waves. Kuru et al. (1995) also note that there is no dramatic change in the mechanisms forming erodible bed waves as the flow rate is increased across the turbulent transition.

The present experiments were focussed on investigating the phenomenon of sand-wavelet generation in an erodible bed for

subcritical laminar flows. Further experiments are required to investigate the development of equilibrium bed configurations for laminar flows. Nevertheless, the development of laminar-flow sand waves subsequent to initial generation would not be expected to be as for alluvial sand waves, lee eddies and turbulence being noted to play a significant role in the later development of the alluvial flow waves.

Conclusions

In contrast to the results of Tison (1949), the present work indicates that stable bed waves can form in subcritical laminar open-channel flows. As for alluvial flows, wavelets (the first waves formed on the bed) generated for laminar open-channel flows are found to be of a preferred wavelength, this length being relatively insensitive to the characteristics of the applied flow and primarily a function of the size of the sediment. The relation $(\lambda/d)Re_{*c}^{0.2} = 10^{2.5}$ of Coleman and Melville (1996) describing alluvial sand-wavelet lengths does not also apply to wavelets forming in laminar open-channel flows. Instead, wavelet lengths for turbulent and laminar open-channel flows over beds of quartz and lightweight sediments of $d = 0.2$ mm to $d = 1.6$ mm can simply be described by $\lambda = 175d^{0.75}$, where λ and d are expressed in millimetres.

The similarities between the bed-wavelet lengths, profiles and generation processes for alluvial and laminar open-channel flows indicate a common generation mechanism for these wavelets. With wavelets forming in the absence of turbulent flow structures, it appears likely that wavelets are generated by an instability within the motion of the granular bed material or by a form of shear layer instability. Analytical descriptions of wavelet generation need to be revised in accordance with the present results, particularly such approaches relying on a turbulent description of the flow, and also approaches predicting wavelet lengths to scale significantly with flow characteristics. The respective development processes for bed waves growing from wavelets in alluvial and laminar open-channel flows exhibit some similarities, but are essentially different owing to essentially different flow structures acting on the waves as they grow from what appear to be the same seed wavelets. For alluvial flows, it is contended that different flow system instability mechanisms can act on the same wavelets at subsequent development stages to provide the two separate types of equilibrium bed forms, ripples and dunes, from the same wavelets. Respective rates of wave generation and development are significantly less for laminar flows as compared to alluvial flows owing to the relative viscosities of the fluids.

Further experimental and theoretical investigations are warranted to determine: the degree to which the present laminar flow sand waves are equivalent to such waves occurring for alluvial flows; and whether sand wavelets can be generated in laminar flows for coarser non-rippling sediments, which, based on alluvial flow results, would be expected to form dunes rather than ripples. The understanding of bed-form mechanics needs to be further revised in light of the findings of these studies.

Acknowledgements

The writers would like to acknowledge both the encouragement given and also comments made by Associate Professor Bruce Melville in regard to these studies. The writers would also like to thank Glen Cornelius for providing his experimental data. In addition, the first writer is grateful for the resources provided by the Iowa Institute of Hydraulic Research of the University of Iowa to enable the present work to be completed during his visit there.

Notations

d	representative sediment size
d_g	geometric mean sediment size, $d_g = (d_{84}d_{16})^{0.5}$
d_{16}	sediment size for which 16% by weight of the sediment is finer
d_{50}	median sediment size
d_{84}	sediment size for which 84% by weight of the sediment is finer
Fr	centreline Froude number, $Fr = U_{ave}/(gh)^{0.5}$
g	gravitational acceleration
h	flow depth
r	channel hydraulic radius
$r(\lambda)$	autocorrelation estimate for a wave of length λ
Re	channel Reynolds number, $Re = 4U_{ave}r/\nu$
Re_*	grain Reynolds number, $Re_* = d_g u_* / \nu$
Re_{*c}	critical grain Reynolds number, $Re_{*c} = du_{*c} / \nu$
s	sediment specific gravity
T	temperature
u_*	shear velocity at the bed level
u_{*c}	critical shear velocity for sediment entrainment determined using Shields diagram
U_{ave}	depth-averaged centreline velocity, average velocity
λ	sand-wavelet length
ν	fluid kinematic viscosity
θ	dimensionless shear stress, $\theta = u_*^2 / [(s-1)gd]$
θ_c	dimensionless critical shear stress, $\theta_c = u_{*c}^2 / [(s-1)gd]$
ρ	fluid density
σ_g	geometric standard deviation of sediment sizes, $\sigma_g = (d_{84}/d_{16})^{0.5}$

References/Bibliographie

- BAAS, J. H. (1993). "Dimensional analysis of current ripples in recent and ancient depositional environments." *Geologica Ultraiectina*, Faculteit Aardwetenschappen der Rijksuniversiteit, Utrecht, Netherlands, 106.
- CHORLTON, F. (1967). "Textbook of fluid dynamics." Van Nostrand Co., Princeton, New Jersey, U.S.A.
- COLEMAN, S. E. (1991). "The mechanics of alluvial stream bed forms." *PhD thesis*, The University of Auckland, Auckland, New Zealand.
- COLEMAN, S. E. (1997). "Ultrasonic measurement of sediment bed profiles." *Proc., 27th Congress of the International Association for Hydraulic Research*, San Francisco, California, USA, August, B221–B226.
- COLEMAN, S. E. and CORNELIUS, G. A. (1998). "Alluvial sand wavelets." *Proc., 7th International Symposium on River Sedimentation*, Hong Kong, China, December, 65–71.

- COLEMAN, S. E., ELING, B. and TWISE, G. (1998). "Sand-wave formation in laminar open-channel flow." *Proc., 7th International Symposium on River Sedimentation*, Hong Kong, China, December, 73–78.
- COLEMAN, S. E. and FENTON, J. D. (1996). "Potential flow instability theory and bed forms." *Proc., North American Water and Environment Congress '96*, ASCE, Anaheim, California, USA, June, 6 pages.
- COLEMAN, S. E. and MELVILLE, B. W. (1994). "Bed-form development." *J. Hyd. Engrg., ASCE*, 120(5), 544–560.
- COLEMAN, S. E. and MELVILLE, B. W. (1996). "Initiation of bed forms on a flat sand bed." *J. Hyd. Engrg., ASCE*, 122(6), 301–310.
- CORNELIUS, G. A. (1997). "Initial development of alluvial stream bed forms." *Project report*, Department of Civil and Resource Engineering, The University of Auckland, Auckland, New Zealand.
- ELING, B. (1997). "Sand-wave development in a rectangular channel under uniform laminar flow." *Project report*, Department of Civil and Resource Engineering, The University of Auckland, Auckland, New Zealand.
- JAIN, S. C. and KENNEDY, J. F. (1971). "The growth of sand waves." *Proc., Int. Symp. on Stochastic Hydr.*, Pittsburgh University Press, Pittsburgh, Pa., U.S.A., 449–471.
- KURU, W. C., LEIGHTON, D. T. and MCCREADY, M. J. (1995). "Formation of waves on a horizontal erodible bed of particles." *Int. J. Multiphase Flow*, Vol. 21, No. 6, 1123–1140.
- NAKAGAWA, H. and TSUJIMOTO, T. (1984). "Spectral analysis of sand bed instability." *J. Hyd. Engrg., ASCE*, 110(4), 467–483.
- RAICHLIN, F. and KENNEDY, J. F. (1965). "The growth of sediment bed forms from an initially flattened bed." *Proc., 11th Cong. Int. Assn. for Hyd. Res.*, Leningrad, U.S.S.R., Vol. 3, Paper 3.7.
- RAUDKIVI, A. J. (1990). "Loose boundary hydraulics." 3rd Ed., Pergamon Press, Inc., New York, New York, U.S.A.
- RAUDKIVI, A. J. (1997). "Ripples on stream bed." *J. Hyd. Engrg., ASCE*, 123(1), 58–64.
- RAUDKIVI, A. J. and WITTE, H. H. (1990). "Development of bed features." *J. Hyd. Engrg., ASCE*, 116(9), 1063–1079.
- TISON, L. J. (1949). "Origine des Ondes de Sable et des Bancs de Sable sous l'Action des Courants." *Report II-13, 3rd Congress I.A.H.R.*, Grenoble, France.
- TWISE, G. (1996). "Sand-wave formation in a rectangular channel under uniform laminar flow." *Project report*, Department of Civil and Resource Engineering, The University of Auckland, Auckland, New Zealand.
- WHITE, S. J. (1970). "Plane bed threshold of fine grained sediments." *Nature*, Vol. 228, No. 5267, 152–153.
- YALIN, M. S. (1972). "Mechanics of sediment transport." Pergamon Press, Inc., New York, New York, U.S.A.
- YALIN, M. S. (1992). "River mechanics." Pergamon Press, Inc., New York, New York, U.S.A.